

Article

Characteristics, Secondary Transformation Potential and Health Risks of Atmospheric Volatile Organic Compounds in an Industrial Area in Zibo, East China

Baolin Wang¹, Ziang Li¹, Zhenguo Liu¹, Yuchun Sun¹, Chen Wang^{1,*}, Yang Xiao^{2,*}, Xiaochen Lu¹, Guihuan Yan³ and Chongqing Xu^{1,3}

¹ School of Environmental Science and Engineering, Qilu University of Technology (Shandong Academy of Sciences), Jinan 250353, China

² Zibo Eco-Environmental Monitoring Center of Shandong Province, Zibo 250101, China

³ Ecology Institute of Shandong Academy of Sciences, Qilu University of Technology (Shandong Academy of Sciences), Jinan 250103, China

* Correspondence: wangchen@qlu.edu.cn (C.W.); xiaoyangsdzb@163.com (Y.X.)

Abstract: As an important anthropogenic source of volatile organic compounds (VOCs), industrial emissions have a significant impact on air quality and human health. In this study, the characteristics, chemical reactivities, and health risks of VOCs around an industrial park in Zibo were analyzed at two sampling sites. The results showed that the concentrations of total VOCs at Dongzhang Community (DZ) and Special School (SS) sites were 113.12 ppb and 139.40 ppb, respectively, with oxygenated VOCs (OVOCs) as the most abundant species, accounting for 42–45%, followed by alkanes (19.3–19.6%). Diurnal variation of OVOCs exhibited noticeable peaks at 3:00, which may be related to the nighttime sneaky emissions of some enterprises. OVOCs were the species with the highest photochemical activity, with an average contribution of 56.5% to OH radical loss rate and 57% to ozone generation. In addition, OVOCs contributed 40% to secondary organic aerosol formation potential at both sites, second only to aromatics (55%). Acrolein and 1,2-dichloropropane presented the highest non-cancer and cancer risks to human health. The results highlight the importance of OVOCs in some industrial areas.

Keywords: industrial park; volatile organic compounds; ozone formation potential; secondary organic aerosol formation potential; health risk assessment



Citation: Wang, B.; Li, Z.; Liu, Z.; Sun, Y.; Wang, C.; Xiao, Y.; Lu, X.; Yan, G.; Xu, C. Characteristics, Secondary Transformation Potential and Health Risks of Atmospheric Volatile Organic Compounds in an Industrial Area in Zibo, East China. *Atmosphere* **2023**, *14*, 158. <https://doi.org/10.3390/atmos14010158>

Academic Editors: Chinmoy Sarkar and Roger Seco

Received: 29 November 2022

Revised: 7 January 2023

Accepted: 9 January 2023

Published: 10 January 2023



Copyright: © 2023 by the authors. Licensee MDPI, Basel, Switzerland. This article is an open access article distributed under the terms and conditions of the Creative Commons Attribution (CC BY) license (<https://creativecommons.org/licenses/by/4.0/>).

1. Introduction

Volatile organic compounds (VOCs) are defined as organic species with saturated vapor pressure higher than 13.33 Pa under standard atmospheric conditions [1]. VOCs include a large variety of species, such as oxygenated VOCs (OVOCs), chlorinated VOCs, and aromatic hydrocarbons (benzene, toluene, ethylbenzene, xylene), which are emitted from a wide variety of natural and anthropogenic sources. The main anthropogenic sources of VOCs include vehicle emissions, combustion, industrial emissions, fuel evaporation and solvent usage [2,3]. Some of the biogenic VOCs are emitted mainly by natural sources, such as vegetation, oceans, and soils [4,5]. Compared with anthropogenic emissions, biogenic contribution is usually minor in urban atmospheres [6]. Many VOCs are important precursors leading to the formation of troposphere ozone (O₃) and secondary organics in particulate matter (PM) [7]. In addition, some VOC are toxic and have adverse effects on human health [8–11].

Liu et al. [12] found that industrial emissions were the primary anthropogenic source, accounting for 55% of anthropogenic VOCs. Emissions of industrial VOCs in China increased from 8777 kt in 2011 to 12,446 kt in 2018, with an average annual growth rate of 5.2% [13]. OVOCs were a significant contributor to total VOCs (TVOCs) in industrial

areas [14–16]. Studies have been conducted to evaluate characteristics and sources of VOCs in some industrial parks in China. An et al. [17] found that VOCs showed significant diurnal variations in an industrial zone in Nanjing, with high concentrations at night and low concentrations during the daytime. Shao et al. [18] found that industrial and solvent use contributed the highest proportion of VOCs in the Yangtze River Delta, followed by vehicle emissions. Jia [19] analyzed the characteristics of NMHCs in different atmospheric environments in Lanzhou. Their results showed that the concentration of NMHCs in industrial zones was 3–11 times higher than that in urban areas. However, most previous studies have not performed simultaneous monitoring of OVOCs.

Epidemiological studies indicated that people living near industrial areas (i.e., within a 5 km radius) had a greater risk of respiratory symptoms than those far from industrial areas [20,21]. Zheng et al. [22] found that acrolein and 1,3-butadiene had the highest carcinogenic risk in a petrochemical industrial park. Benzene, carbon tetrachloride and naphthalene were the major cancer risk species in the urban areas of Calgary, Canada [8]. Carbon tetrachloride, benzene, and 1,3-butadiene were the main cancer risk species in Vancouver, Canada [23]. Benzo(a)pyrene had the highest cancer risk in a steel industrial zone in Korea, followed by formaldehyde and benzene [24].

Zibo is a large industry-driven cluster city of about 6000 km² and 4.7 million population and is located in the middle of Shandong Province and the central area of North China Plain. Zibo has intensive and comprehensive industrial categories, with industry contributing about 50% of its annual gross domestic product [25,26]. According to Zibo's 2018 annual emission inventory, the total anthropogenic VOC emission was approximately 100 kt, which was dominated by chemical processing (62.9 kt) [27]. In recent years, Zibo has been suffering from severe PM_{2.5} and O₃ pollution [25,27]. However, few reports are available about VOCs in Zibo.

In this study, the samples of VOCs were collected by canister and 2,4-dinitrophenylhydrazine (DNPH) cartridges at two sites around an industrial park in Zibo, and VOCs were analyzed by gas chromatography mass spectrometer/flame ionization detector (GC–MS/FID) and high-performance liquid chromatography (HPLC). The concentrations, diurnal variations, secondary transformation potential, sources and health risks of VOCs were analyzed. This study can provide theoretical support for the establishment of air pollution control strategies in Zibo.

2. Materials and Methods

2.1. Site Description

The study was conducted in an industrial area of Zibo, which is located in the central Shandong Province (Figure 1). Two sampling sites were set up around an industrial park, the Dongzhang Community (DZ) and the Special School (SS) sites, respectively. This industrial park is a cluster of industrial chains led by organic raw material, pharmaceutical, and new material industries, and is the largest production base of chloroacetic acid, aspirin, ibuprofen and ankyrin in the world. It is surrounded by mixed commercial, transportation, and residential areas.

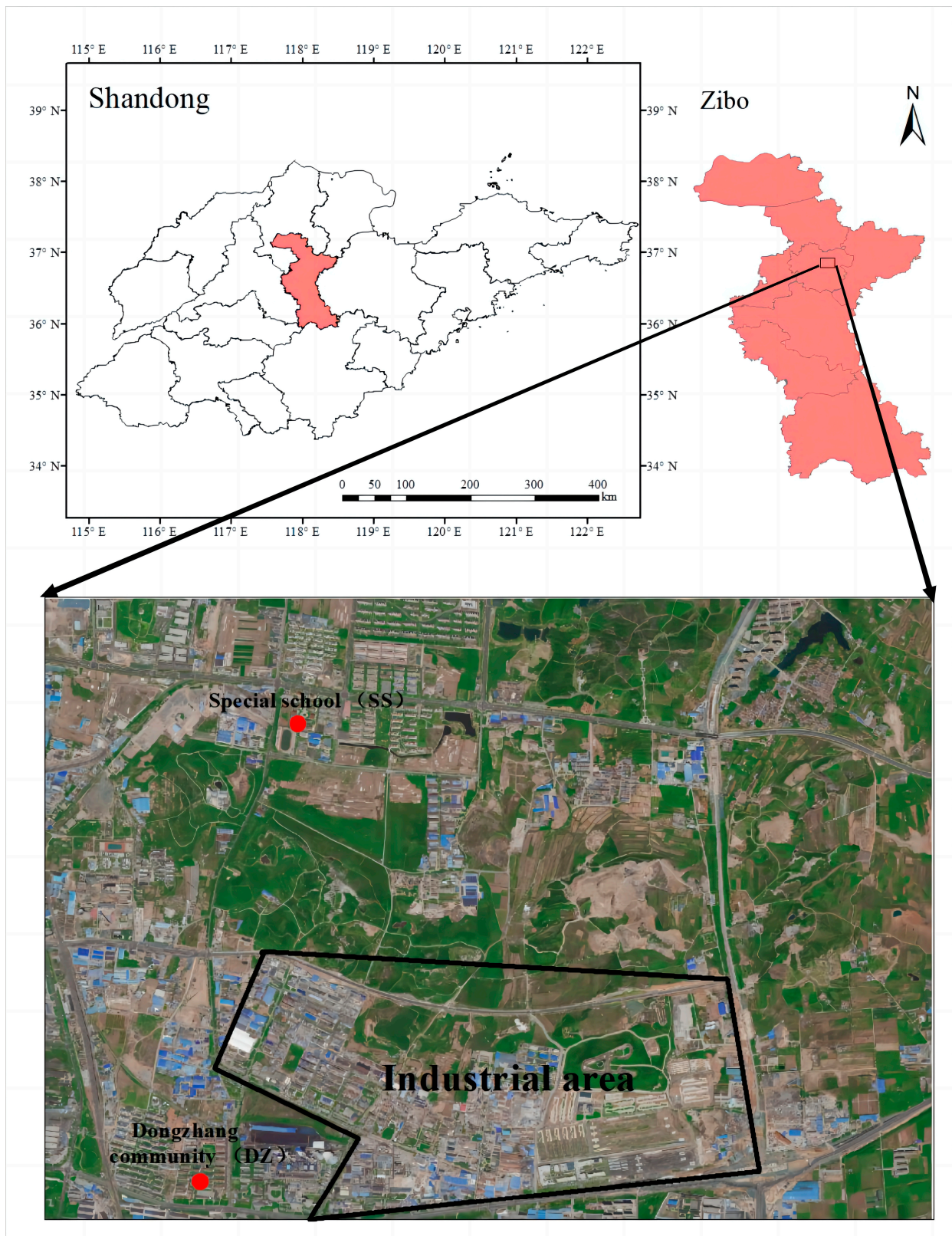


Figure 1. Location of sampling site and the surrounding areas in the industrial area.

2.2. Sampling and Measurement Methods

The field measurements were performed 15–17 December 2020. Ambient air samples from DZ and SS sites were collected in SUMMA canisters with flow restriction devices

to control the sampling flow rate (15 mL/min for 3 h). In addition, atmospheric OVOCs were collected simultaneously at both sites using DNPH cartridges for a period of 3 h per sample. Eight samples were collected per day at each site. Ambient air samples from the SUMMA canister were analyzed by GC–MS/FID. The gas samples were pre-concentrated by an ultra-low-temperature system and then thermally desorbed into the separation and detection system. The C2–C5 hydrocarbons were separated on an Al₂O₃/KCl PLOT column and detected by FID detector, and the C5–C12 compounds were separated on a DB-624 column and detected by MS detector. The samples collected by DNPH were first eluted with acetonitrile for the derivatives and then analyzed by HPLC with UV detector.

2.3. Quality Assurance and Quality Control (QA/QC)

Before sampling, all SUMMA canisters were cleaned by repeated evacuation and filling with high-purity nitrogen. After cleaning, the 10% canisters were refilled with pure nitrogen and stored in the laboratory for at least 24 h to check for contamination. Calibration curves for each standard gas were established using a high-precision diluter at six different concentrations (0, 1, 2, 5, 10 and 20 ppb). The correlation coefficients (R) of the standard curves for all species exceeded 0.99. The method detection limits (MDL) ranged from 0.002 to 0.05 ppb. The concentrations of more than 98% of the target compounds were above the MDL, and the precision was within 15%, which proved the stability and reliability of the instrument and method.

To evaluate the feasibility of the DNPH–HPLC method for OVOC measurement, the sampling and analytical method were assessed for relevant quality assurance parameters, including the leakage of the sampling system, sampling flow error, method detection limit, precision, standard recovery, elution efficiency, and sample stability. The results showed that the method is reliable and can be used in the following studies.

2.4. L_{OH}, OFP and SOAP Calculation

Most of the oxidation of organics in the troposphere is performed by reaction with OH radicals [28]. The OH radical loss rate (L_{OH}) is commonly used to describe the photochemical reactivity of VOCs [29–31]. The L_{OH} of VOCs is the multiplication of their concentration in the atmosphere and the OH radical reaction rate constant [29].

L_{OH} is calculated using Equation (1):

$$L_{OH_i} = K_{OH_i} \times [VOC_i] \quad (1)$$

where L_{OH_i} is the OH radical loss rate of the *i*th VOC Species (s^{−1}), K_{OH_i} is the rate coefficient for the reaction of the *i*th VOCs species with OH radicals (cm³ · (molecule s)^{−1}), and [VOC_{*i*}] is the measured concentration of the *i*th species (molecule · cm^{−3}). The K_{OH_i} values are derived from Atkinson [32].

The contribution of VOCs to ozone formation varies depending on their photochemical reactivity. To comprehensively estimate the contribution of each VOCs species to ozone formation potential (OFP), the maximum incremental reactivity (MIR) method was used in this study to quantify the OFP of VOCs.

OFP is calculated using Equation (2) [33]:

$$OFP_i = MIR_i \times [VOC_i] \quad (2)$$

where OFP_{*i*} is the ozone formation potential of the *i*th VOC species, MIR_{*i*} is the MIR scale of the *i*th VOC species, and [VOC_{*i*}] is the measured concentration of the *i*th species (μg/m³). The MIR coefficients for the VOCs species are obtained from Carter [33].

Secondary organic aerosol (SOA) is one of the important components of PM_{2.5} [34]. As key VOCs species are important precursors of SOA, their identification is crucial to control PM_{2.5} pollution. Estimating the secondary organic aerosol formation potential (SOAP) is often used to obtain the relative contribution of VOCs to SOA formation.

The SOAP was calculated using the following equation [35]:

$$\text{SOAP}_i = [\text{VOC}]_i \times \text{SOAP}^*_i \quad (3)$$

where SOAP_i represents the potential for secondary organic aerosol generation of the i th VOC species, SOAP^*_i represents the potential for SOA generation of the i th VOC species relative to an equivalent mass of toluene, and $[\text{VOC}]_i$ represents the monitored concentration ($\mu\text{g}/\text{m}^3$) of the i th VOC species. The SOAP^*_i coefficient is the latest research result of Derwent [35].

2.5. Health Risk Assessment

Inhalation is the most significant pathway of human exposure to air pollutants, other than ingestion and dermal absorption [10,36]. Therefore, the health risks of VOCs associated with inhalation were assessed in this study area using the standard USEPA methodology. The hazard ratio (HR) is used to assess the non-carcinogenic risk, which is the ratio of the daily concentration ($[\text{VOC}]_i$, $\mu\text{g}/\text{m}^3$) to the reference concentration of a specific VOC (RfC_i , $\mu\text{g}/\text{m}^3$) [37]. As shown in Equation (4):

$$\text{HR}_i = \frac{[\text{VOC}]_i}{\text{RfC}_i} \quad (4)$$

The lifetime cancer risk (LCR) method is generally used to assess the cancer risk of VOCs [37]. The LCR represents the increased probability of cancer in humans due to exposure to carcinogenic compounds, which is calculated by multiplying the daily concentration of each VOC ($[\text{VOC}]_i$, $\mu\text{g}/\text{m}^3$) by the unit risk (URF_i , $(\mu\text{g}/\text{m}^3)^{-1}$) [37]:

$$\text{LCR}_i = [\text{VOC}]_i \times \text{URF}_i \quad (5)$$

Excel, Origin and ArcGIS were used for data analysis and graphic plotting in this study.

3. Results and Discussion

3.1. General Characteristics of VOCs

A total of 77 VOC species were monitored by GC-MS/FID together with DNPH-HPLC in this study, including 19 alkanes, 8 alkenes (including isoprene), 15 aromatic hydrocarbons, 8 halogenated hydrocarbons, 22 OVOCs, acetylene, naphthalene, carbon disulfide, acetonitrile, and acrylonitrile. The average concentrations of each species are shown in Table S1. The TVOCs concentrations at DZ and SS sites were 113.12 ppb and 139.4 ppb, respectively. The higher TVOCs concentration at the SS site may be attributed to the fact that the SS site was located in the downwind direction of the industrial park (the wind direction was mostly south during the sampling period) and close to the main road.

Figure 2 shows the contributions of each group to TVOCs. OVOCs were the predominant group at both DZ and SS sites during the sampling period, with 45.9% and 42.8% of the TVOCs, respectively. The second dominant group was alkanes, accounting for 19.6% at the DZ site and 19.2% at the SS site, followed by halogenated hydrocarbons (13.4% and 17.4%, respectively). The results were consistent with the chemical compositions of VOCs collected from most enterprises in this industrial park during the sampling period.

As shown in Table 1, concentrations of TVOCs in different industrial sites were compared. The results demonstrated that TVOCs concentrations in this study were significantly higher than those in Beijing [38], Nanjing [17], Shanghai [39], Houston [40], Taiyuan [11] and Wuhan [22], especially OVOCs. This is probably due to the more comprehensive VOC monitoring instruments used in this study, with the simultaneous use of DNPH tubes for aldehydes and ketones on the basis of GC-MS/FID (standard gases including PAMS, TO15, and domestic OVOC standard gases), which resulted in more OVOCs species measured in this study. Some previous studies considered only non-methane hydrocarbon species, ignoring the effects of OVOCs [17,18,40,41].

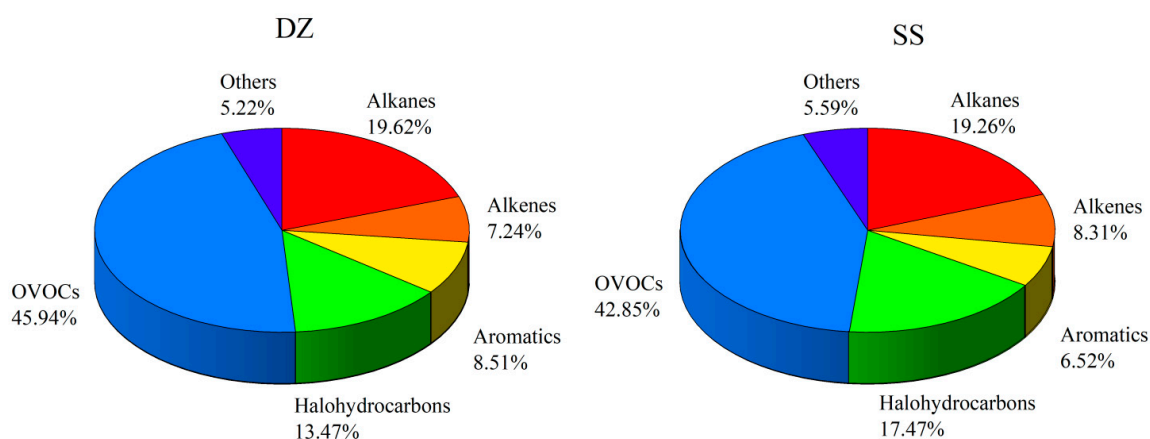


Figure 2. Composition of different groups of VOCs.

The sum of the top 10 VOC species at the DZ and SS sites accounted for 52.16% and 56.86% of the TVOC concentrations, respectively. The top 10 species at the DZ site during the observation period were propanal (13.56 ppb), vinyl chloride (8.01 ppb), ethanol (6.75 ppb), and propane (6.48 ppb), etc. The top 10 species at the SS site were propanal (18.61 ppb), dichloromethane (17.16 ppb), propane (8.97 ppb), and ethane (6.14 ppb), etc. From the above results, the dominant species in this industrial area are mainly OVOCs such as propanal and ethanol, C2~C3 alkanes, and halogenated hydrocarbons such as dichloromethane. Figure 3 shows the comparison of individual VOCs with high concentrations at both sites during the observation period. The measured average concentrations of 1,2-dichloroethane, acetylene, benzene, toluene, and vinyl chloride were higher at the DZ site, and acetone, acetonitrile, acrolein and propanal showed lower levels at the DZ site. The results indicated the difference of emission sources for VOCs at the DZ and SS sites.

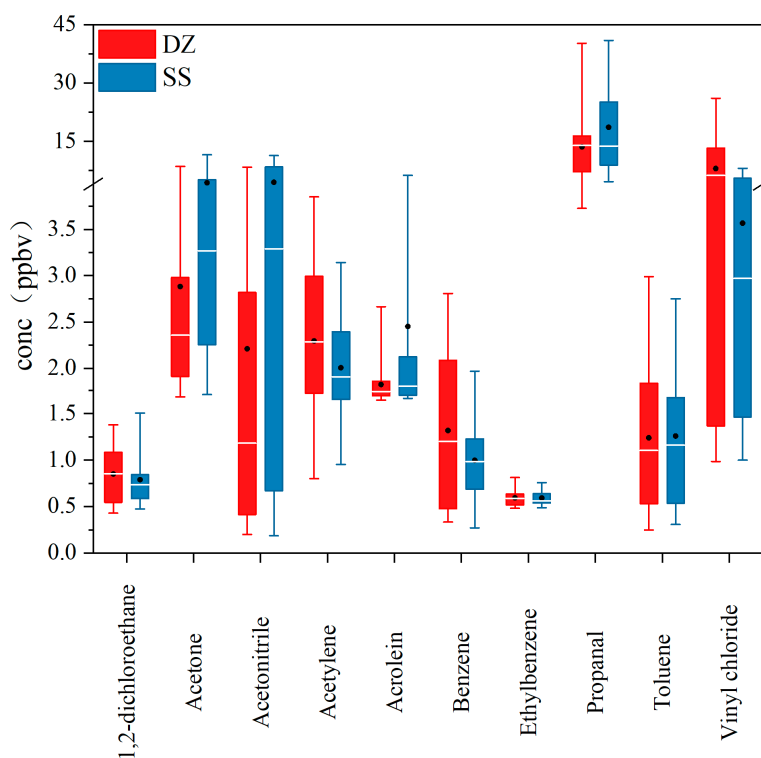


Figure 3. Comparison of VOC concentrations at DongZhang community (DZ) and Special School (SS) sites. The upper and lower bars indicate the maximum and minimum values. Lines inside boxes show the median value, and black dots show the mean values.

Table 1. Comparison of VOC concentrations at different industrial sites (unit: ppb).

| Sampling Site | Alkanes | Alkenes | Aromatics | Halohydrocarbons | OVOcs | Others | TVOCs | Reference |
|------------------|---------------|--------------|---------------|------------------|---------------|-------------|---------------|---------------------------|
| Beijing, China | 53.27 ± 11.8 | 2.55 ± 1.76 | 29.79 ± 89.18 | — | 7.35 ± 2.94 | 1.32 ± 1.02 | 94.3 ± 157.8 | Liu et al. (2022) [38] |
| Nanjing, China | 19.6 | 11.1 | 9.7 | — | — | 3.2 | 43.5 | An et al. (2014) [17] |
| Shanghai, China | 39.3 | 16.87 | 18.92 | 11.75 | 3.61 | 3.01 | 94.14 | Zhang et al. (2018) [39] |
| Taiyuan, China | 18.14 ± 11.8 | 5.79 ± 4.91 | 8.51 ± 7.69 | 1.78 ± 1.52 | — | 4 ± 3.41 | 38.43 ± 24.2 | Li et al. (2020) [11] |
| Wuhan, China | 41.4 | 19.9 | 8.17 | 11.2 | 14.7 | 4.54 | 99.91 | Zheng et al. (2020) [22] |
| Weinan, China | 29.27 | 9.8 | 7.2 | — | 6.98 | 21 | 73.4 | Li et al. (2022) [42] |
| Xian, China | 21.3 | 8.59 | 7.6 | — | 8.34 | 16.44 | 62.3 | Li et al. (2022) [42] |
| Nanjing, China | 14.98 ± 12.72 | 7.35 ± 5.93 | 9.06 ± 6.64 | — | — | 3.02 ± 2.01 | 34.41 ± 25.2 | Shao et al. (2016) [18] |
| Houston, USA | 28.01 | 3.84 | 1.75 | — | — | — | 33.6 | Bavand et al. (2022) [40] |
| Taiwan, China | 6.25 | 1.54 | 1.82 | — | — | 0.83 | 10.44 | Chen et al. (2019) [41] |
| Zibo, China (DZ) | 22.19 ± 8.96 | 8.19 ± 4.47 | 9.62 ± 2.03 | 15.23 ± 9.02 | 51.97 ± 16.92 | 5.9 ± 2.69 | 113.1 ± 34.94 | This study |
| Zibo, China (SS) | 26.85 ± 14.67 | 11.58 ± 9.71 | 9.09 ± 1.74 | 24.36 ± 28.74 | 59.73 ± 21.34 | 7.78 ± 4.39 | 139.39 ± 74 | This study |

3.2. Diurnal Variations of VOCs

The diurnal variations of VOCs may be influenced by the boundary layer, local emissions, photochemical reactions and air quality transport [21]. Generally, the diurnal variation of VOCs showed a decreasing trend during the daytime due to the elevated boundary layer and enhanced photochemical depletion [43]. Figure 4 shows the diurnal variations of alkanes, aromatics and OVOCs at two sites. In this study, isobutane and n-butane showed similar diurnal variation patterns at both sites, with elevated concentrations during the traffic morning rush hour (6:00–9:00), minimum values in the afternoon due to the photochemical reaction consumption, and peak values at 21:00. The diurnal trends of ethylbenzene and o-xylene were significantly different between the two sites, with peaks at 15:00 at the SS site, probably influenced by strong local emissions from industrial processes. For acetone, there were unexpected peak values at 3:00 at both sites, possibly related to the nighttime sneaky emissions of some enterprises.

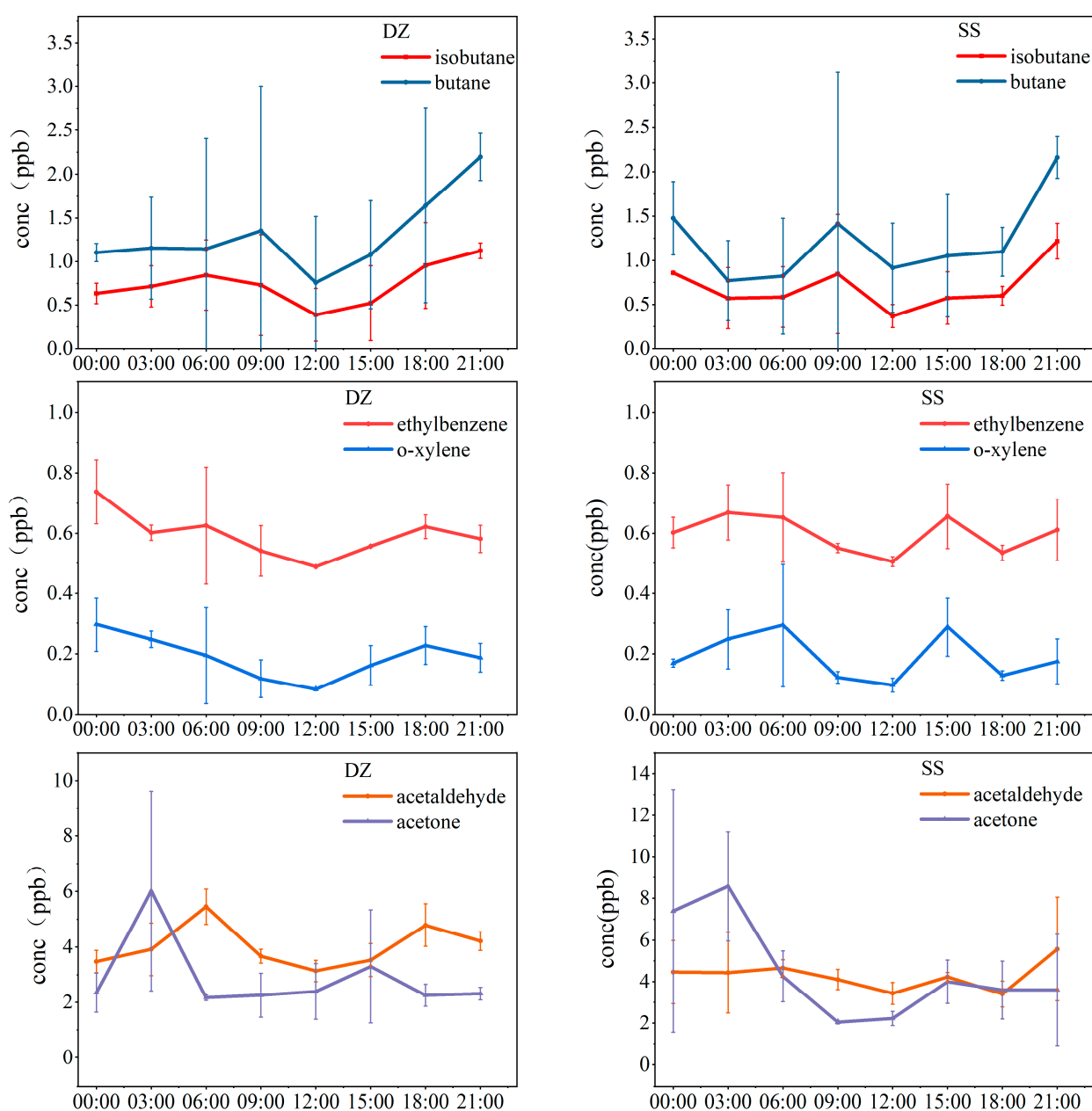


Figure 4. Diurnal variations of VOCs at DZ and SS sites.

3.3. Secondary Transformation Potential of VOCs

3.3.1. VOCs–OH Reactivity and Ozone Formation Potential

Previous studies have shown that VOC concentrations were not proportional to their ozone formation potential [30,44]. To better understand the reactivity and O₃ generation potential of individual VOCs, the L_{OH} method was used to evaluate the VOCs reactivities, and the MIR method was applied to assess the contributions of VOCs to OFP in this study.

During the sampling period of this study, the OFP of the measured VOCs at the DZ and SS sites was 1138 and 1313 µg/m³, respectively. As shown in Figure 5, OVOCs were the major contributors to OFP at both sites, accounting for 56% and 58% of the total OFP at DZ and SS, respectively, followed by aromatics (17–19%) and alkenes (14–18%). The concentrations of alkanes and halocarbons were much higher than those of alkenes and aromatics, but the photochemical reaction activity of alkanes and halocarbons was lower, so their contributions to OFP were lower than those of alkenes and aromatics. Alkanes and halocarbons accounted for only 4–5% and 2–6% of the total OFP, respectively.

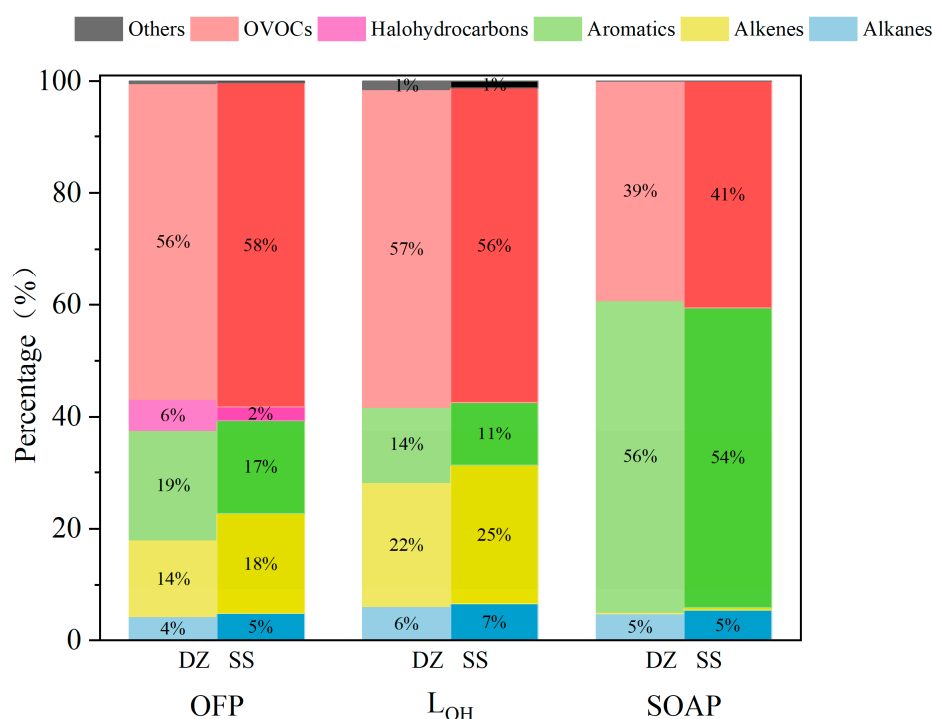


Figure 5. Contributions of VOCs groups to the total OFP, L_{OH} and SOAP at DZ and SS sites.

The total L_{OH} for all the measured VOCs was 26.6 s⁻¹ and 31.7 s⁻¹ for the DZ and SS sites, respectively. The results of the contribution of each VOCs group to L_{OH} were similar to those of OFP, with OVOCs as the most important component of L_{OH} (56–57%), followed by alkenes (22–15%), aromatics (11–14%) and alkanes (6–7%). Halogenated hydrocarbons with very low photochemical reactivity were not involved in the calculation of L_{OH} in this study. This implies that there was no significant relationship between VOCs concentration and photochemical reactivity, whereas the photochemical reactivity of VOCs was significantly related to the contribution of VOCs to O₃ generation, and the contribution to OFP was greater for species with higher photochemical reactivity.

The top 10 VOC species that contributed most to OFP and L_{OH} were mainly C2–C6 OVOCs (propanal, acetaldehyde, butanal, hexanal, pentanal and butenal) and C2–C4 alkenes (1,3-butadiene, ethylene and propene. These species contributed 51–57% of the total OFP and 64–68% of the total L_{OH} at the DZ and SS sites. Propanal was the species with the highest contribution to OFP and L_{OH} at both sites (Table S2), with an average contribution of 24% and 27%, respectively. Propanal is commonly used as solvent,

antifreeze, lubricant, and dehydrating agent [45]. Based on the simultaneous studies, the measured propanal was emitted mainly from pharmaceutical companies in this industrial park.

3.3.2. SOA Formation Potential

VOCs are important precursors of secondary gaseous pollutants such as SOA [46]. Previous studies indicated that organic aerosols contributed 30.5% of PM_{2.5} mass concentration in the North China Plain, and SOA accounted for 44% of organic aerosols [46]. Therefore, identification of key VOC species in the generation of SOA is essential to reduce atmospheric PM_{2.5} concentrations. Among the 77 VOCs in this study, 43 VOCs exhibited SOA generation potential, including 14 aromatics, 11 alkanes, 6 alkenes, 11 OVOCs, and acetylene. The SOAP at the DZ and SS sites was 7499 and 7392 µg/m³, respectively. The contributions of different VOC groups to the total SOAP at both sites were shown in Figure 5. Aromatics were the primary contributors to SOAP at both sites, accounting for 54–56% of the total SOAP during the sampling period, followed by OVOCs, accounting for 39–41% of the total SOAP. However, the contributions of alkenes and alkanes were lower, about 5%. Previous studies have shown that aromatics were the major contributors to SOAP, accounting for 92–98.5% in Beijing [47] and 98.41% in Shanghai [48]. The relatively minor contribution of aromatics to the total SOAP in this study may be related to the emission characteristics of VOCs in this industrial park, where concentrations of OVOCs are substantially higher than those of aromatics.

The top 10 VOC species that contributed most to the total SOAP in this study were shown in Figure S1. Benzaldehyde was the species with the most significant contribution to SOAP at both the DZ and the SS site, with an average contribution of 39.3%, while its concentration was only about 2% of the total VOC concentration. Benzaldehyde is an important raw material for pharmaceutical and chemical production [49,50]. Emissions from pharmaceutical companies in the industrial park might have significantly impacted SOA generation in the research area. The alkane n-dodecane was the only alkane in the top 10 SOAP species at the SS site. Except for benzaldehyde and n-dodecane, the top 10 SOAP species were all aromatics at both sites, accounting for 42–47% of the total SOAP.

3.4. Specific VOC Ratios

Different VOCs have different sources and photochemical reactivities in the atmosphere. The ratios of some specific VOCs can be used to preliminarily identify their emission sources [17,51,52]. In this study, the ratios of toluene/benzene (T/B) and propane/ethane were analyzed to initially assess the emission sources of VOCs.

As shown in Figure 6a, the ratio of T/B varies significantly in different emission sources. The ratio of T/B differs in vehicle emission sources based on the vehicle type, ranging from 0.9 ± 0.6 to 2.2 ± 0.5 [53–56]. To reduce the influence of other emission sources on the vehicles, the researchers conducted experiments with diesel and gasoline vehicles in a more concentrated and less convective air tunnel. Therefore, the ratio of T/B in traffic sources should be closer to the results of the tunnel experiments, about 1.5 ± 0.1 [57]. When VOCs were derived mainly from coal and biomass combustion, the T/B ratios ranged from 0.2 to 0.6 [58,59]. The ratio of T/B was higher than 8.8 ± 6.5 in various solvent usage sources [60]. In industrial source emission studies, the T/B ratios varied from 1.4 ± 0.8 to 5.8 ± 3.4 [16,61]. The ratios of T/B at the SS site ranged from 0.65 to 2.75 in this study, with an average of 1.28, which implies that industrial sources and vehicle emissions significantly contributed to benzene and toluene at the site. The ratios of T/B at the DZ site ranged from 0.46 to 1.74, with an average value of 0.86. Vehicle emissions and coal combustion could be important sources of VOCs, since this sampling site was located within a residential area where residents may use coal for heating.

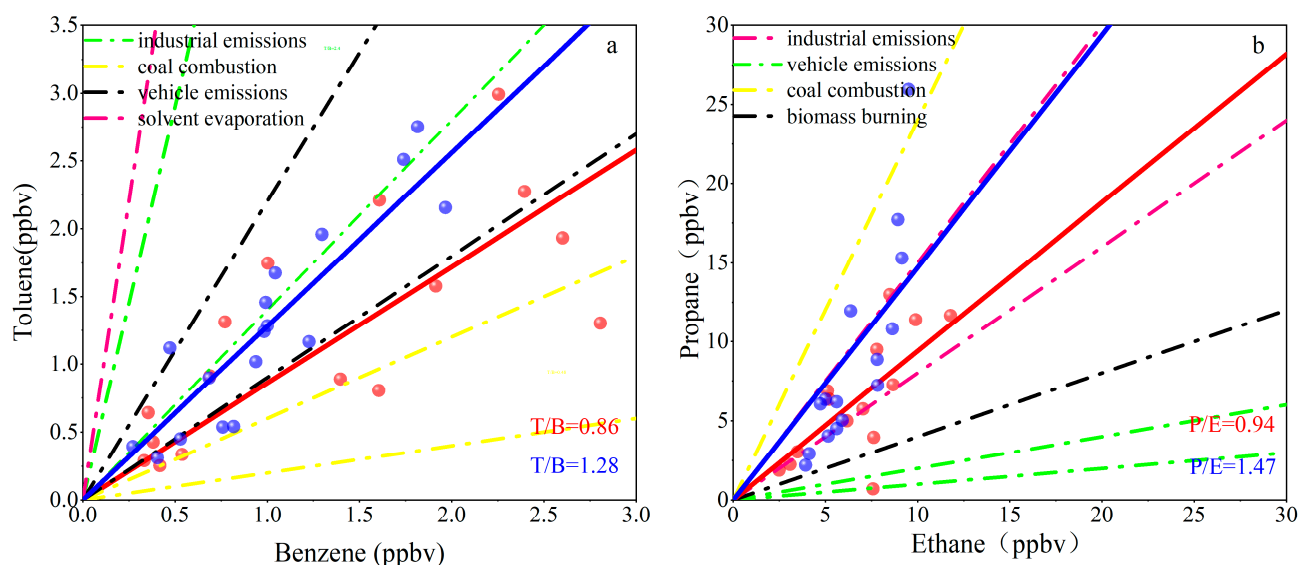


Figure 6. Ratios of toluene/benzene and propane/ethane at the DZ (red) and SS (blue) sites.

Propane/ethane ratios of 0.2–0.4 and 1.5–2.4 were associated with biomass burning and coal combustion [12,62]. The range of 0.1–0.2 and 0.8–1.5 for propane/ethane were considered as vehicle emissions and industrial sources [61,63]. In this study, the average ratios of propane/ethane at DZ and SS sites were 0.94 and 1.27 (Figure 6b), with ratios within the industrial emission interval, indicating that industrial emissions contribute significantly to atmospheric propane and ethane in this area, which was consistent with the sampling sites being located near industrial park.

3.5. Health Risk Assessment of Individual VOC Species

According to the International Agency for Research on Cancer (IARC), cancer VOCs can be classified into group 1 (carcinogenic to humans), group 2A (probably carcinogenic to humans), group 2B (possibly carcinogenic to humans) and group 3 (not classifiable as to its carcinogenicity to humans). In this study, the cancer and non-cancer risks of VOCs species were assessed by inhalation exposure. If the non-cancer risk (HR_i) was lower than 1, it indicated insignificant impact on human health. If the cancer risk (LCR_i) was $>10^{-4}$, 10^{-5} – 10^{-4} , 10^{-6} – 10^{-5} and $<10^{-6}$, VOC species were considered as definite risk, probable risk, possible risk, and negligible risk, respectively [64].

Figure 7a shows the non-cancer risk ratios (HR_i) of 31 VOC species. The average total HR was 28.74 for the DZ and SS sites. Acrolein (HR = 15.23) was the dominant non-cancer HR risk species, which was consistent with studies in the Beijing suburban area [65] and Zhengzhou corporate work area [66]. The average HRs of propanal (5.12), 1,3-butadiene (2.04), n-heptane (1.66), 1,2-dichloropropane (1.16) and naphthalene (1.11) were higher than 1, which may present non-cancer threats to residents within the study area. The HRs of other VOC species were below the acceptable safe level.

Figure 7b shows the cancer risk ratios (LCR_i) of 13 VOC species. The average total LCR was 7.5×10^{-4} for the DZ and SS sites during the sampling time, which demonstrated a relatively high cancer risk in the study area. Group 1 included 1,2-dichloropropane, 1,3-butadiene and naphthalene, which were recognized as definite risks, with mean LCR values of 1.73×10^{-4} , 1.23×10^{-4} and 1.14×10^{-4} , respectively. Group 2B included 1,2-dichloroethane (9.28×10^{-5}), trichloromethane (7.33×10^{-5}), and vinyl chloride (6.83×10^{-5}), which were classified as probable risk. Acrylonitrile (3.94×10^{-5}), benzene (3.57×10^{-5}), acetaldehyde (1.74×10^{-5}) and carbon tetrachloride (2.01×10^{-5}) can also be categorized as group 2B, with possible risk. The LCR values of other VOC species were below 10^{-6} , which were considered as negligible risk.

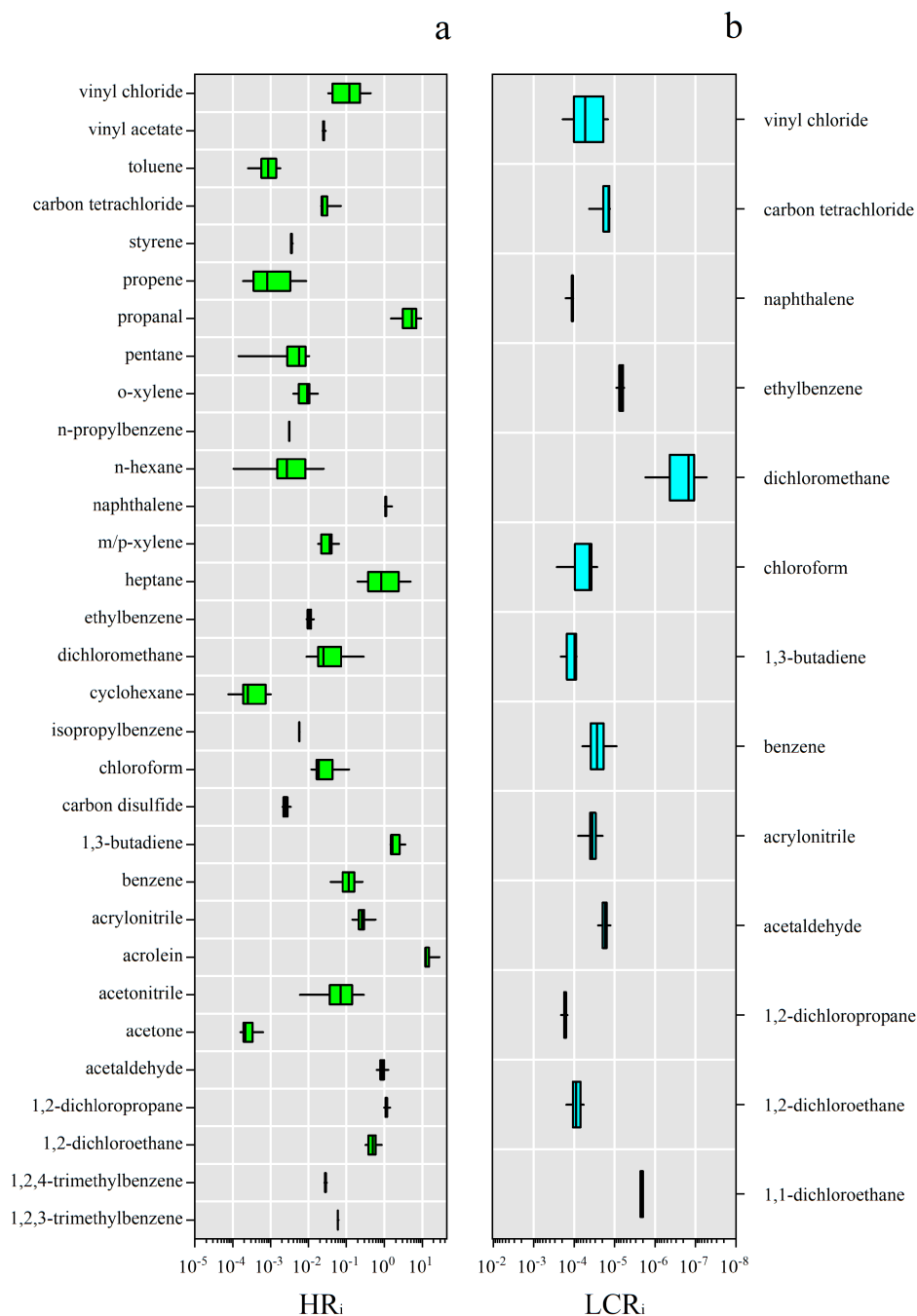


Figure 7. Distributions of non-cancer (a) and cancer (b) risks for individual VOC species. The box plots were constructed according to the 25–75th percentiles and the vertical lines inside the boxes represented the median values.

Cancer and non-cancer risks of specific VOCs in this study were compared with those in previous studies (Table 2). The results indicated that the health risks of VOCs in this study were more serious than those in other cities. In general, acrolein presented the highest non-cancer risk to human health, and 1,2-dichloropropane produced the highest cancer risk in this study, and their concentrations should be reduced to prevent their health risks to nearby residents.

Table 2. Comparison of cancer and non-cancer risks of specific VOCs in different cities.

| Sampling Site | Non-Cancer (HR) | | | Cancer (LCR) | | | Reference | |
|------------------|-----------------|-------------|---------------|---------------|--|--|--|--------------------------|
| | Acrolein | Propanal | Butadiene | Benzene | 1,2-dichloropropane | Benzene | | Vinyl Chloride |
| YRD, China | — | — | 0.113 ± 0.161 | 0.487 ± 0.227 | — | 4.07×10^{-5} | 6.98×10^{-6} | Jia et al. (2021) [67] |
| Beijing, China | 1.33 | — | — | 0.0127 | — | 2.97×10^{-6} | — | Liu et al. (2023) [38] |
| Zhengzhou, China | 3.8 | — | 0.017 | 0.034 | — | 8.0×10^{-6} | 8.3×10^{-7} | Zhang et al. (2021) [66] |
| Hefei, China | — | — | — | 0.296 | — | 9.85×10^{-5} | — | Hu et al. (2018) [9] |
| Xian, China | — | — | 0.0626 | 0.0425 | — | 4.27×10^{-6} | 1.19×10^{-6} | Xu et al. (2021) [7] |
| Harbin, China | — | — | — | 0.011 | — | 1.97×10^{-6} | — | Xuan et al. (2021) [68] |
| Wuhan, China | 22.8 | — | 1.66 | 0.15 | 3.5×10^{-5} | 3.6×10^{-5} | — | Zheng et al. (2020) [22] |
| Tabriz, Iran | — | — | — | 0.107 | — | 7.82×10^{-6} | — | Tohid et al. (2019) [69] |
| Zibo, China | 15.23 ± 10.25 | 5.12 ± 3.88 | 2.04 ± 0.043 | 0.13 ± 0.057 | $1.73 \times 10^{-4} \pm$ 2.64×10^{-5} | $3.07 \times 10^{-5} \pm$ 1.34×10^{-5} | $6.83 \times 10^{-5} \pm$ 2.77×10^{-5} | This study |

4. Conclusions

To better understand the characteristics, secondary transformations, and health risks of VOCs in industrial areas, DZ and SS sites around one of the Zibo industrial parks were selected for the analysis of atmospheric VOCs. The average concentration of TVOCs at the DZ and SS sites was 113.12 and 139.4 ppb, respectively. Both sites exhibited significant OVOCs pollution, with an average contribution of 44% to TVOCs, far exceeding that of the remaining VOCs species. In addition, OVOCs played a major role in photochemical reactions, contributing 57% to OFP and 40% to SOAP. The ratios of T/B and propane/ethane were used to identify sources of VOC. The results indicate that the measured VOCs were influenced mainly by the combination of industrial emissions, vehicle emissions, and coal combustion.

The results of the health risk evaluation showed that the non-cancer risks of acrolein, propanal, 1,3-butadiene, n-heptane, 1,2-dichloropropane and naphthalene were above the safe level ($HR > 1$), and benzene and ethylbenzene were within the acceptable levels recommended by the EPA. The average value of LCR was 5.76×10^{-6} , which exceeded the EPA acceptable risk level ($LCR < 1 \times 10^{-6}$), with 1,2-dichloropropane, 1,3-butadiene and naphthalene as the main cancer risk species. From a health risk perspective, acrolein, 1,2-dichloropropane, 1,3-butadiene, and naphthalene should be considered as priority control VOCs in this study area. This study can provide scientific support for the establishment of air pollution control strategies, and it can provide a reference for governments to develop effective policies to reduce human exposure to environmental VOCs around industrial parks. In the following studies, more VOCs samples around Zibo Industrial Park will be collected for further analysis.

Supplementary Materials: The following supporting information can be downloaded at: <https://www.mdpi.com/article/10.3390/atmos14010158/s1>, Figure S1: Contributions of the top 10 VOCs to the total SOAP at DZ and SS sites; Table S1: Concentrations of each VOC species at DZ and SS sites in Zibo (unit: ppb); Table S2: Top 10 VOC species contributed to L_{OH} and OFP at DZ and SS sites.

Author Contributions: Conceptualization, B.W., C.W. and Y.X.; Validation, B.W., Z.L. (Ziang Li), Z.L. (Zhenguo Liu), Y.S., C.W., Y.X., X.L., G.Y. and C.X.; Investigation, Z.L. (Ziang Li), Z.L. (Zhenguo Liu), Y.S. and X.L.; Data curation, Y.S., X.L., G.Y. and C.X.; Writing—original draft, B.W., Z.L. (Ziang Li) and Z.L. (Zhenguo Liu); Writing—review & editing, B.W. and C.W.; Funding acquisition, B.W., Y.X., G.Y. All authors have read and agreed to the published version of the manuscript.

Funding: This research was funded by the National Natural Science Foundation of China (41905111), Shandong Provincial Natural Science Foundation (ZR2019BD030), Shandong Province Key R & D project (2017GSF17116, 2019GSF109043), the Major Innovation Projects for Science and Education Integration of Qilu University of Technology (Shandong Academy of Science) (2022JBZ02-05) and the Science & Technology Development Plan Projects of Zibo (2017kj010080).

Institutional Review Board Statement: Not applicable.

Informed Consent Statement: Not applicable.

Data Availability Statement: The data presented in this study are available on request from the corresponding author.

Conflicts of Interest: The authors declare no conflict of interest.

References

1. Tai, X.H.; Chook, S.W.; Lai, C.W.; Lee, K.M.; Yang, T.C.K.; Chong, S.; Juan, J.C. Effective photoreduction of graphene oxide for photodegradation of volatile organic compounds. *RSC Adv.* **2019**, *9*, 18076–18086. [[CrossRef](#)]
2. Ilgen, E.; Karfich, N.; Levsen, K.; Angerer, J.; Schneider, P.; Heinrich, J.; Wichmann, H.E.; Dunemann, L.; Begerow, J. Aromatic hydrocarbons in the atmospheric environment: Part I. Indoor versus outdoor sources, the influence of traffic. *Atmos. Environ.* **2001**, *35*, 1235–1252. [[CrossRef](#)]

3. Zhao, L.; Wang, X.; He, Q.; Wang, H.; Sheng, G.; Chan, L.; Fu, J.; Blake, D. Exposure to hazardous volatile organic compounds, PM10 and CO while walking along streets in urban Guangzhou, China. *Atmos. Environ.* **2004**, *38*, 6177–6184. [[CrossRef](#)]
4. Öztürk, N.; Ergenekon, P.; Seçkin, G.; Bayir, S. Spatial Distribution and Temporal Trends of VOCs in a Highly Industrialized Town in Turkey. *Bull. Environ. Contam. Toxicol.* **2015**, *94*, 653–660. [[CrossRef](#)] [[PubMed](#)]
5. Sahu, L.K.; Yadav, R.; Pal, D. Source identification of VOCs at an urban site of western India: Effect of marathon events and anthropogenic emissions. *J. Geophys. Res. Atmos.* **2016**, *121*, 2416–2433. [[CrossRef](#)]
6. Barletta, B.; Meinardi, S.; Rowland, F.S.; Chan, C.Y.; Wang, X.; Zou, S.; Chan, L.Y.; Blake, D.R. Volatile organic compounds in 43 Chinese cities. *Atmos. Environ.* **2005**, *39*, 5979–5990. [[CrossRef](#)]
7. Xu, H.; Li, Y.; Feng, R.; He, K.; Ho, S.S.H.; Wang, Z.; Ho, K.F.; Sun, J.; Chen, J.; Wang, Y.; et al. Comprehensive characterization and health assessment of occupational exposures to volatile organic compounds (VOCs) in Xi'an, a major city of northwestern China. *Atmos. Environ.* **2020**, *246*, 118085. [[CrossRef](#)]
8. Bari, M.A.; Kindziarski, W.B. Ambient volatile organic compounds (VOCs) in Calgary, Alberta: Sources and screening health risk assessment. *Sci. Total Environ.* **2018**, *631–632*, 627–640. [[CrossRef](#)]
9. Hu, R.; Liu, G.; Zhang, H.; Xue, H.; Wang, X. Levels, characteristics and health risk assessment of VOCs in different functional zones of Hefei. *Ecotoxicol. Environ. Saf.* **2018**, *160*, 301–307. [[CrossRef](#)]
10. Yao, X.Z.; Ma, R.C.; Li, H.J.; Wang, C.; Zhang, C.; Yin, S.S.; Wu, D.; He, X.Y.; Wang, J.; Zhan, L.T.; et al. Assessment of the major odor contributors and health risks of volatile compounds in three disposal technologies for municipal solid waste. *Waste Manag.* **2019**, *91*, 128–138. [[CrossRef](#)]
11. Li, J.; Li, H.; He, Q.; Guo, L.; Zhang, H.; Yang, G.; Wang, Y.; Chai, F. Characteristics, sources and regional inter-transport of ambient volatile organic compounds in a city located downwind of several large coke production bases in China. *Atmos. Environ.* **2020**, *233*, 117573. [[CrossRef](#)]
12. Liu, Y.; Shao, M.; Fu, L.; Lu, S.; Zeng, L.; Tang, D. Source profiles of volatile organic compounds (VOCs) measured in China: Part I. *Atmos. Environ.* **2008**, *42*, 6247–6260. [[CrossRef](#)]
13. Liang, X.; Sun, X.; Xu, J.; Ye, D. Improved emissions inventory and VOCs speciation for industrial OFP estimation in China. *Sci. Total Environ.* **2020**, *745*, 140838. [[CrossRef](#)]
14. Mozaffar, A.; Zhang, Y.L.; Lin, Y.C.; Xie, F.; Fan, M.Y.; Cao, F. Measurement report: High contributions of halocarbon and aromatic compounds to atmospheric volatile organic compounds in an industrial area. *Atmos. Chem. Phys.* **2021**, *21*, 18087–18099. [[CrossRef](#)]
15. Na, K.; Kim, Y.P.; Moon, K.C.; Moon, I.; Fung, K. Concentrations of volatile organic compounds in an industrial area of Korea. *Atmos. Environ.* **2001**, *35*, 2747–2756. [[CrossRef](#)]
16. Shi, J.; Deng, H.; Bai, Z.; Kong, S.; Wang, X.; Hao, J.; Han, X.; Ning, P. Emission and profile characteristic of volatile organic compounds emitted from coke production, iron smelt, heating station and power plant in Liaoning Province, China. *Sci. Total Environ.* **2015**, *515–516*, 101–108. [[CrossRef](#)]
17. An, J.; Zhu, B.; Wang, H.; Li, Y.; Lin, X.; Yang, H. Characteristics and source apportionment of VOCs measured in an industrial area of Nanjing, Yangtze River Delta, China. *Atmos. Environ.* **2014**, *97*, 206–214. [[CrossRef](#)]
18. Shao, P.; An, J.; Xin, J.; Wu, F.; Wang, J.; Ji, D.; Wang, Y.S. Source apportionment of VOCs and the contribution to photochemical ozone formation during summer in the typical industrial area in the Yangtze River Delta, China. *Atmos. Res.* **2016**, *176–177*, 64–74. [[CrossRef](#)]
19. Jia, C. Characteristics and Chemical Behaviors of Atmospheric Non-Methane Hydrocarbons in Lanzhou Valley, Western China. Master's Thesis, Lanzhou University, Lanzhou, China, 2018. (In Chinese).
20. Nadal, M.; Mari, M.; Schuhmacher, M.; Domingo, J.L. Multi-compartmental environmental surveillance of a petrochemical area: Levels of micropollutants. *Environ. Int.* **2009**, *35*, 227–235. [[CrossRef](#)]
21. Hsu, C.Y.; Chiang, H.C.; Shie, R.H.; Ku, C.H.; Lin, T.Y.; Chen, M.J.; Chen, N.T.; Chen, Y.C. Ambient VOCs in residential areas near a large-scale petrochemical complex: Spatiotemporal variation, source apportionment and health risk. *Environ. Pollut.* **2018**, *240*, 95–104. [[CrossRef](#)]
22. Zheng, H.; Kong, S.; Yan, Y.; Chen, N.; Yao, L.; Liu, X.; Wu, F.; Cheng, Y.; Niu, Z.; Zheng, S.; et al. Compositions, sources and health risks of ambient volatile organic compounds (VOCs) at a petrochemical industrial park along the Yangtze River. *Sci. Total Environ.* **2019**, *703*, 135505. [[CrossRef](#)] [[PubMed](#)]
23. Xiong, Y.; Bari, A.; Xing, Z.; Du, K. Ambient volatile organic compounds (VOCs) in two coastal cities in western Canada: Spatiotemporal variation, source apportionment, and health risk assessment. *Sci. Total Environ.* **2019**, *706*, 135970. [[CrossRef](#)]
24. Baek, K.M.; Kim, M.J.; Kim, J.Y.; Seo, Y.K.; Baek, S.O. Characterization and health impact assessment of hazardous air pollutants in residential areas near a large iron-steel industrial complex in Korea. *Atmos. Pollut. Res.* **2020**, *11*, 1754–1766. [[CrossRef](#)]
25. Li, H.; Ma, Y.; Duan, F.; He, K.; Zhu, L.; Huang, T.; Kimoto, T.; Ma, X.; Ma, T.; Xu, L.; et al. Typical winter haze pollution in Zibo, an industrial city in China: Characteristics, secondary formation, and regional contribution. *Environ. Pollut.* **2017**, *229*, 339–349. [[CrossRef](#)] [[PubMed](#)]
26. Qiping, R. Circular Economy Action Programs and Countermeasures for Small and Medium-sized Resource-based Cities of China-Case Study of Zibo City of Shandong Province. *Energy Procedia* **2011**, *5*, 2183–2188. [[CrossRef](#)]

27. Li, K.; Wang, X.; Li, L.; Wang, J.; Liu, Y.; Cheng, X.; Xu, B.; Wang, X.; Yan, P.; Li, S.; et al. Large variability of O₃-precursor relationship during severe ozone polluted period in an industry-driven cluster city (Zibo) of North China Plain. *J. Clean. Prod.* **2021**, *316*, 128252. [[CrossRef](#)]
28. Edwards, P.M.; Brown, S.S.; Roberts, J.M.; Ahmadov, R.; Banta, R.M.; Degouw, J.A.; Dubé, W.P.; Field, R.A.; Flynn, J.H.; Gilman, J.B.; et al. High winter ozone pollution from carbonyl photolysis in an oil and gas basin. *Nature* **2014**, *514*, 351–354. [[CrossRef](#)]
29. Atkinson, R.; Arey, J. Atmospheric Degradation of Volatile Organic Compounds. *Chem. Rev.* **2003**, *103*, 4605–4638. [[CrossRef](#)]
30. Zou, Y.; Deng, X.J.; Zhu, D.; Gong, D.C.; Wang, H.; Li, F.; Tan, H.B.; Deng, T.; Mai, B.R.; Liu, X.T.; et al. Characteristics of 1 year of observational data of VOCs, NO_x and O₃ at a suburban site in Guangzhou, China. *Atmos. Chem. Phys.* **2015**, *15*, 6625–6636. [[CrossRef](#)]
31. Winkler, J.; Blank, P.; Glaser, K.; Gomes, J.A.G.; Habram, M.; Jambert, C.; Jaeschke, W.; Konrad, S.; Kurtenbach, R.; Lenschow, P.; et al. Ground-based and airborne measurements of nonmethane hydrocarbons in BERLIOZ: Analysis and selected results. *J. Atmos. Chem.* **2002**, *42*, 465–492. [[CrossRef](#)]
32. Atkinson, R.; Baulch, D.L.; Cox, R.A.; Crowley, J.N.; Hampson, R.F.; Hynes, R.G.; Jenkin, M.E.; Rossi, M.J.; Troe, J.; Subcommittee, I. Evaluated kinetic and photochemical data for atmospheric chemistry: Volume II—Gas phase reactions of organic species. *Atmos. Chem. Phys.* **2006**, *6*, 3625–4055. [[CrossRef](#)]
33. Carter, W.P. Development of a condensed SAPRC-07 chemical mechanism. *Atmos. Environ.* **2010**, *44*, 5336–5345. [[CrossRef](#)]
34. Rao, Z.; Chen, Z.; Liang, H.; Huang, L.; Huang, D. Carbonyl compounds over urban Beijing: Concentrations on haze and non-haze days and effects on radical chemistry. *Atmos. Environ.* **2016**, *124*, 207–216. [[CrossRef](#)]
35. Derwent, R.G.; Jenkin, M.; Utembe, S.; Shallcross, D.E.; Murrells, T.P.; Passant, N.R. Secondary organic aerosol formation from a large number of reactive man-made organic compounds. *Sci. Total Environ.* **2010**, *408*, 3374–3381. [[CrossRef](#)] [[PubMed](#)]
36. Nie, E.; Zheng, G.; Ma, C. Characterization of odorous pollution and health risk assessment of volatile organic compound emissions in swine facilities. *Atmos. Environ.* **2020**, *223*, 117233. [[CrossRef](#)]
37. Ramírez, N.; Cuadras, A.; Rovira, E.; Borrull, F.; Marcé, R.M. Chronic risk assessment of exposure to volatile organic compounds in the atmosphere near the largest Mediterranean industrial site. *Environ. Int.* **2012**, *39*, 200–209. [[CrossRef](#)]
38. Liu, C.; Xin, Y.; Zhang, C.; Liu, J.; Liu, P.; He, X.; Mu, Y. Ambient volatile organic compounds in urban and industrial regions in Beijing: Characteristics, source apportionment, secondary transformation and health risk assessment. *Sci. Total Environ.* **2023**, *855*, 158873. [[CrossRef](#)] [[PubMed](#)]
39. Zhang, Y.; Li, R.; Fu, H.; Zhou, D.; Chen, J. Observation and analysis of atmospheric volatile organic compounds in a typical petrochemical area in Yangtze River Delta, China. *J. Environ. Sci.* **2018**, *71*, 233–248. [[CrossRef](#)] [[PubMed](#)]
40. Sadeghi, B.; Pouyaei, A.; Choi, Y.; Rappenglueck, B. Influence of seasonal variability on source characteristics of VOCs at Houston industrial area. *Atmos. Environ.* **2022**, *277*, 119077. [[CrossRef](#)]
41. Chen, C.H.; Chuang, Y.C.; Hsieh, C.C.; Lee, C.S. VOC characteristics and source apportionment at a PAMS site near an industrial complex in central Taiwan. *Atmos. Pollut. Res.* **2019**, *10*, 1060–1074. [[CrossRef](#)]
42. Li, J.; Deng, S.; Tohti, A.; Li, G.; Yi, X.; Lu, Z.; Liu, J.; Zhang, S. Spatial characteristics of VOCs and their ozone and secondary organic aerosol formation potentials in autumn and winter in the Guanzhong Plain, China. *Environ. Res.* **2022**, *211*, 113036. [[CrossRef](#)]
43. Sarkar, C.; Sinha, V.; Kumar, V.; Rupakheti, M.; Panday, A.; Mahata, K.S.; Rupakheti, D.; Kathayat, B.; Lawrence, M.G. Overview of VOC emissions and chemistry from PTR-TOF-MS measurements during the SusKat-ABC campaign: High acetaldehyde, isoprene and isocyanic acid in wintertime air of the Kathmandu Valley. *Atmos. Chem. Phys.* **2016**, *16*, 3979–4003. [[CrossRef](#)]
44. Shi, Y.; Xi, Z.; Simayi, M.; Li, J.; Xie, S. Scattered coal is the largest source of ambient volatile organic compounds during the heating season in Beijing. *Atmos. Chem. Phys.* **2020**, *20*, 9351–9369. [[CrossRef](#)]
45. Ashizawa, A.; Roney, N.; Taylor, J. Toxicological Profile for Acrolein. Available online: <https://stacks.cdc.gov/view/cdc/6954> (accessed on 21 October 2022).
46. Huang, R.J.; Zhang, Y.; Bozzetti, C.; Ho, K.F.; Cao, J.J.; Han, Y.; Daellenbach, K.R.; Slowik, J.G.; Platt, S.M.; Canonaco, F.; et al. High secondary aerosol contribution to particulate pollution during haze events in China. *Nature* **2014**, *514*, 218–222. [[CrossRef](#)]
47. Zhan, J.; Feng, Z.; Liu, P.; He, X.; He, Z.; Chen, T.; Wang, Y.; He, H.; Mu, Y.; Liu, Y. Ozone and SOA formation potential based on photochemical loss of VOCs during the Beijing summer. *Environ. Pollut.* **2021**, *285*, 117444. [[CrossRef](#)]
48. Wang, S.; Zhao, Y.; Han, Y.; Li, R.; Fu, H.; Gao, S.; Duan, Y.; Zhang, L.; Chen, J. Spatiotemporal variation, source and secondary transformation potential of volatile organic compounds (VOCs) during the winter days in Shanghai, China. *Atmos. Environ.* **2022**, *286*, 119203. [[CrossRef](#)]
49. Kholkina, E.; Mäki-Arvela, P.; Lozachmeur, C.; Barakov, R.; Shcherban, N.; Murzin, D.Y. Prins cyclisation of (–)-isopulegol with benzaldehyde over ZSM-5 based micro-mesoporous catalysts for production of pharmaceuticals. *Chin. J. Catal.* **2019**, *40*, 1713–1720. [[CrossRef](#)]
50. Sowbna, P.R.; Yadav, G.D.; Ramkrishna, D. Population balance modeling and simulation of liquid-liquid-liquid phase transfer catalyzed synthesis of mandelic acid from benzaldehyde. *AIChE J.* **2012**, *58*, 3799–3809. [[CrossRef](#)]
51. Monod, A.; Sive, B.C.; Avino, P.; Chen, T.; Blake, D.R.; Rowland, F.S. Monoaromatic compounds in ambient air of various cities: A focus on correlations between the xylenes and ethylbenzene. *Atmos. Environ.* **2001**, *35*, 135–149. [[CrossRef](#)]

52. Li, B.; Ho, S.S.H.; Gong, S.; Ni, J.; Li, H.; Han, L.; Yang, Y.; Qi, Y.; Zhao, D. Characterization of VOCs and their related atmospheric processes in a central Chinese city during severe ozone pollution periods. *Atmos. Chem. Phys.* **2019**, *19*, 617–638. [[CrossRef](#)]
53. Wang, J.; Jin, L.; Gao, J.; Shi, J.; Zhao, Y.; Liu, S.; Jin, T.; Bai, Z.; Wu, C.Y. Investigation of speciated VOC in gasoline vehicular exhaust under ECE and EUDC test cycles. *Sci. Total Environ.* **2013**, *445–446*, 110–116. [[CrossRef](#)]
54. Yao, Z.; Shen, X.; Ye, Y.; Cao, X.; Jiang, X.; Zhang, Y.; He, K. On-road emission characteristics of VOCs from diesel trucks in Beijing, China. *Atmos. Environ.* **2015**, *103*, 87–93. [[CrossRef](#)]
55. Liu, Y.; Song, M.; Liu, X.; Zhang, Y.; Hui, L.; Kong, L.; Zhang, Y.; Zhang, C.; Qu, Y.; An, J.; et al. Characterization and sources of volatile organic compounds (VOCs) and their related changes during ozone pollution days in 2016 in Beijing, China. *Environ. Pollut.* **2019**, *257*, 113599. [[CrossRef](#)]
56. Song, M.; Li, X.; Yang, S.; Yu, X.; Zhou, S.; Yang, Y.; Chen, S.; Dong, H.; Liao, K.; Chen, Q.; et al. Spatiotemporal variation, sources, and secondary transformation potential of volatile organic compounds in Xi'an, China. *Atmos. Chem. Phys.* **2021**, *21*, 4939–4958. [[CrossRef](#)]
57. Deng, C.; Jin, Y.; Zhang, M.; Liu, X.; Yu, Z. Emission Characteristics of VOCs from On-Road Vehicles in an Urban Tunnel in Eastern China and Predictions for 2017–2026. *Aerosol Air Qual. Res.* **2018**, *18*, 3025–3034. [[CrossRef](#)]
58. Karl, T.G.; Christian, T.J.; Yokelson, R.J.; Artaxo, P.; Hao, W.M.; Guenther, A. The Tropical Forest and Fire Emissions Experiment: Method evaluation of volatile organic compound emissions measured by PTR-MS, FTIR, and GC from tropical biomass burning. *Atmos. Chem. Phys.* **2007**, *7*, 5883–5897. [[CrossRef](#)]
59. Wang, S.; Wei, W.; Du, L.; Li, G.; Hao, J. Characteristics of gaseous pollutants from biofuel-stoves in rural China. *Atmos. Environ.* **2009**, *43*, 4148–4154. [[CrossRef](#)]
60. Yuan, B.; Shao, M.; Lu, S.; Wang, B. Source profiles of volatile organic compounds associated with solvent use in Beijing, China. *Atmos. Environ.* **2010**, *44*, 1919–1926. [[CrossRef](#)]
61. Mo, Z.; Shao, M.; Lu, S.; Qu, H.; Zhou, M.; Sun, J.; Gou, B. Process-specific emission characteristics of volatile organic compounds (VOCs) from petrochemical facilities in the Yangtze River Delta, China. *Sci. Total Environ.* **2015**, *533*, 422–431. [[CrossRef](#)]
62. Zhang, Y.; Shao, M.; Lin, Y.; Luan, S.; Mao, N.; Chen, W.; Wang, M. Emission inventory of carbonaceous pollutants from biomass burning in the Pearl River Delta Region, China. *Atmos. Environ.* **2013**, *76*, 189–199. [[CrossRef](#)]
63. Zhang, Q.; Wu, L.; Fang, X.; Liu, M.; Zhang, J.; Shao, M.; Lu, S.; Mao, H. Emission factors of volatile organic compounds (VOCs) based on the detailed vehicle classification in a tunnel study. *Sci. Total Environ.* **2017**, *624*, 878–886. [[CrossRef](#)]
64. Sexton, K.; Linder, S.H.; Marko, D.; Bethel, H.; Lupo, P. Comparative Assessment of Air Pollution-Related Health Risks in Houston. *Environ. Health Perspect.* **2007**, *115*, 1388–1393. [[CrossRef](#)]
65. Yang, Y.; Ji, D.; Sun, J.; Wang, Y.; Yao, D.; Zhao, S.; Yu, X.; Zeng, L.; Zhang, R.; Zhang, H.; et al. Ambient volatile organic compounds in a suburban site between Beijing and Tianjin: Concentration levels, source apportionment and health risk assessment. *Sci. Total Environ.* **2019**, *695*, 133889. [[CrossRef](#)]
66. Zhang, D.; He, B.; Yuan, M.; Yu, S.; Yin, S.; Zhang, R. Characteristics, sources and health risks assessment of VOCs in Zhengzhou, China during haze pollution season. *J. Environ. Sci.* **2021**, *108*, 44–57. [[CrossRef](#)]
67. Jia, H.; Gao, S.; Duan, Y.; Fu, Q.; Che, X.; Xu, H.; Wang, Z.; Cheng, J. Investigation of health risk assessment and odor pollution of volatile organic compounds from industrial activities in the Yangtze River Delta region, China. *Ecotoxicol. Environ. Saf.* **2020**, *208*, 111474. [[CrossRef](#)]
68. Xuan, L.; Ma, Y.; Xing, Y.; Meng, Q.; Song, J.; Chen, T.; Wang, H.; Wang, P.; Zhang, Y.; Gao, P. Source, temporal variation and health risk of volatile organic compounds (VOCs) from urban traffic in Harbin, China. *Environ. Pollut.* **2020**, *270*, 116074. [[CrossRef](#)]
69. Tohid, L.; Sabeti, Z.; Sarbakhsh, P.; Benis, K.Z.; Shakerkhatibi, M.; Rasoulzadeh, Y.; Rahimian, R.; Darvishali, S. Spatiotemporal variation, ozone formation potential and health risk assessment of ambient air VOCs in an industrialized city in Iran. *Atmos. Pollut. Res.* **2018**, *10*, 556–563. [[CrossRef](#)]

Disclaimer/Publisher's Note: The statements, opinions and data contained in all publications are solely those of the individual author(s) and contributor(s) and not of MDPI and/or the editor(s). MDPI and/or the editor(s) disclaim responsibility for any injury to people or property resulting from any ideas, methods, instructions or products referred to in the content.